Exploring the fission barrier of ^{235}U

A. Oberstedt[1,*] and S. Oberstedt[2]

[1]*Extreme Light Infrastructure - Nuclear Physics (ELI-NP), Horia Hulubei National Institute for Physics and Nuclear Engineering (IFIN-HH), 077125 Bucharest-Magurele, Romania*

[2]*European Commission, Joint Research Centre (JRC), 2440 Geel, Belgium*

(Received 30 March 2021; accepted 20 July 2021; published 11 August 2021)

In this work we have reexamined the shape isomer in ^{235}U. Reanalyzing data from a previous experiment gave a half-life of $T_{1/2} = (11 \pm 3)$ ms and a cross section for populating the isomer of $\sigma_{\rm iso} = (12 \pm 1)$ μb. Combining these new results with measured properties of fission fragments from the reaction ^{234}U(n, f) allowed extracting parameters describing the outer fission barrier. The deduced barrier parameters are $E_B = (5.7 \pm 0.6)$ MeV and $\hbar\omega_B = (0.5 \pm 0.1)$ MeV for the height and curvature, respectively, as well as the energy of the superdeformed ground state $E_{II} = (2.4 \pm 0.6)$ MeV. Separate barrier parameters for the standard-1 and standard-2 fission modes have been estimated, too. Finally, the results obtained in this work have been successfully tested for their plausibility.

DOI: 10.1103/PhysRevC.104.024611

I. INTRODUCTION

Isomeric fission is a consequence of a multihumped fission barrier, which in turn is a result of superposing microscopic shell corrections to the macroscopic liquid drop model [1]. This is described in several review papers [2–4] as well as in Ref. [5]. At that time a shape isomer in ^{235}U was not known yet, although its existence and half-life had already been predicted [6]. An experimental verification was not obtained until many years later in a neutron-induced fission experiment on ^{234}U at JRC Geel with quasimonoenergetic neutrons of $E_n =$ 0.95 and 1.27 MeV. By using a twin Frisch-grid ionization chamber and a chopped beam, both pulse height and time (the latter relative to the time structure of the neutron pulses) of the fission events could be recorded. This allowed an unambiguous distinction between prompt and isomeric fission. The data was analyzed and some properties of the shape isomer in ^{235}U were estimated [7]. Recently, we became aware of rather new, complementing experimental data for the reaction ^{234}U(n, f) [8,9] and the existence of an alternative way of determining half-lives [10]. Therefore we found it worthwhile to revisit the previously taken data. For information about the experiment we refer to Ref. [7].

II. DATA ANALYSIS: TIME DISTRIBUTIONS

Since the half-life of the shape isomer in ^{235}U was expected to be in the millisecond region, from model calculations [6] as well as according to semiempirical formulas [11–13], the pulse frequency in the experiment was chosen to be 50, 100, and 150 Hz. With a duty cycle of 30%, this corresponds to time ranges of 14, 7, and 4.7 ns, respectively. During the measurements the latter turned out to be too short, which is why that run was aborted after a short while and the data taken so far was not used. The determination of half-lives from radioactive decay data may be achieved in different ways, of which two were in principle applicable here. One possibility is to fit an experimentally obtained decay curve with an exponential; another is based on contracting the time range by using a ^{2}log time scale, as suggested in Ref. [10]. There it is shown that investigating exponential decays by this method is advantageous and achieves better precision. After applying a ^{2}log time scale, i.e. binning the detected decay times in intervals exponentially increasing with measuring time, the resulting distribution is described by

$$I(t) = I_0 \times 2^{-t/T_{1/2}}[1 - 2^{-t/T_{1/2}}], \tag{1}$$

with t and $T_{1/2}$ denoting time and half-life, respectively. In this work the latter method is applied to the previously taken data and the results are given below. In accordance with Ref. [10], the time bins are defined by $t_n = t_0\, a^n$. Because of the time ranges covered in the experiment the following values are chosen: $t_0 = 7$ ms, $a = 2$ and $n = -6, -5, \ldots$. Figure 1 shows the experimental time distributions from the three settings with $E_n = 0.95$ MeV (100 Hz) and $E_n = 1.27$ MeV (50 and 100 Hz), normalized to the same measuring time. The line represents the fit according to Eq. (1). As result, a half-life of $T_{1/2} = (11 \pm 3)$ ms and a total number of isomeric fission events of $N_{\rm iso} = 79 \pm 10$ were obtained, corresponding to the position and to four times the value of the maximum of the fit, respectively [10]. Dividing $N_{\rm iso}$ with the corresponding number of prompt fission events gives a probability $P_{\rm iso} = (10 \pm 1) \times 10^{-6}$ and, by multiplying with the fission cross section, a cross section $\sigma_{\rm iso} = (12 \pm 1)$ μb for isomeric fission. The same fitting procedure was also applied to the data for each neutron energy alone by keeping the half-life above. Those results, together with others, are listed below.

*Corresponding author: andreas.oberstedt@eli-np.ro

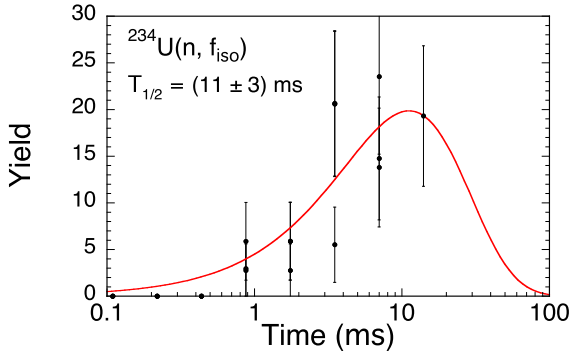

FIG. 1. Decay time spectrum of the shape isomer in ^{235}U. The experimental data, together with statistical uncertainties, are compared to the result of a fit according to Eq. (1).

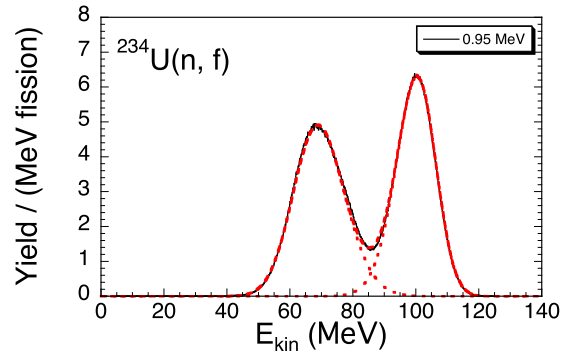

FIG. 2. Post-neutron kinetic energy spectrum of fission fragments from ^{234}U(n, f) at $E_n = 0.95$ MeV, corresponding to prompt fission. In addition, the fit of two skew Gaussians is shown as dotted lines.

III. DATA ANALYSIS: PULSE HEIGHT DISTRIBUTIONS

Until now, the measured pulse-height distributions from neither prompt nor isomeric fission of ^{235}U* from Ref. [7] could be analyzed, apart from counting the number of the events. A calibration from pulse height to post-neutron kinetic energy, i.e., kinetic energy of the fission fragment after neutron emission, cannot be performed, if only one of the fragments is detected (see, e.g., Ref. [14]). Fortunately, the reaction ^{234}U(n, f) was studied again some years later for incident neutron energies $E_n = 0.2$–5.0 MeV [8], hence including the neutron energies in Ref. [7] and this work. Since post-neutron kinetic energy ($E_{\mathrm{kin,post}}$) spectra were provided for $E_n = 0.9$ and 1.0 MeV [15], they could be used to calibrate the pulse-height spectrum for $E_n = 0.95$ MeV. This was done by fitting energy and pulse-height spectra with two skew Gaussians,

$$Y(E_{\mathrm{kin}}) = \sum_i \frac{A_i}{\sqrt{2\pi}\,\sigma_i} \exp\left(\frac{(E_{\mathrm{kin}} - E_{\mathrm{kin},i})^2}{2\sigma_i^2}\right) \times \left[1 + \mathrm{erf}\left\{\alpha_i\left(\frac{E_{\mathrm{kin}} - E_{\mathrm{kin},i}}{\sqrt{2}\sigma_i}\right)\right\}\right], \qquad (2)$$

with $i = heavy, light$ and $A_{\mathrm{heavy}} = A_{\mathrm{light}}$ to ensure that heavy and light fragments amount the same yield. Equation (2) represents a generalization of skew-normal distributions [16] with skewness parameters α_i after transformation $E_{\mathrm{kin}} \rightarrow (E_{\mathrm{kin}} - E_{\mathrm{kin},i})/\sigma_i$. The calibrated post-neutron energy spectrum at $E_n = 0.95$ MeV is depicted in Fig. 2, together with the result of the fit according to Eq. (2). The agreement is very good, which allows determination of the average kinetic energies (post-neutron emission) for the heavy and light fragments, $\overline{E}_{\mathrm{kin,heavy}}$(post) and $\overline{E}_{\mathrm{kin,light}}$(post) from the fit, and finally the corresponding average total kinetic energy $\overline{\mathrm{TKE}}$(post) as the sum of both. For all prompt fission events analyzed here, a value of $\overline{\mathrm{TKE}}$(post) = (169.22 ± 0.12) was found. The average neutron energy of $\overline{E}_n = 1.16$ MeV is obtained by weighting $E_n = 0.95$ and 1.27 MeV with the respective number of detected prompt events. Due to the extremely low number of isomeric fission events, this fitting method cannot be applied to their fragment energy distribution. Therefore another method was needed to determine $\overline{\mathrm{TKE}}$(post) for isomeric fission. By applying this to the prompt fission fragments, an estimate for a systematic uncertainty can be obtained. We chose to divide the energy spectrum into two parts, both containing half of the total number of events, For each part the average kinetic energy is determined and added, leading to $\overline{\mathrm{TKE}}$(post) = 168.9 MeV. In this case, the statistical uncertainty, i.e. standard deviation, amounts to some MeV, which does not reflect the real accuracy. However, a systematic uncertainty of 0.3 MeV can be deduced from both $\overline{\mathrm{TKE}}$(post) values that can be applied to the isomeric fission events, too. Figure 3 shows the 50 detected isomeric fission fragments in a two-dimensional plot of time vs kinetic energy. The logarithmic time scale according to Fig. 1 is chosen to emphasize the regions of heavy and light fragments. The deduced average total kinetic energy for isomeric fission of ^{235}U is then the sum of the average kinetic energy of both fragment groups, leading to $\overline{\mathrm{TKE}}$(post) = (167.0 ± 0.3) MeV. The given uncertainty is the systematic one as explained above.

The purpose of determining $\overline{\mathrm{TKE}}$ for prompt and isomeric fission is to extract information about some properties of the double-humped fission barrier by using the dependence of $\overline{\mathrm{TKE}}$ on the excitation energy E^* of the compound nucleus. Obviously, isomeric fission corresponds to fission at an exci-

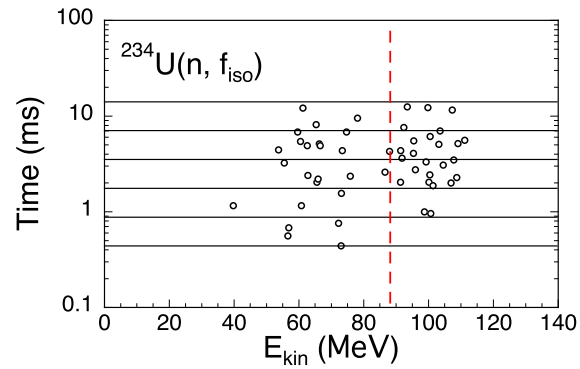

FIG. 3. Two-dimensional presentation of isomeric fission events by their time and kinetic energy. The solid lines indicate the time bins in Fig. 1, while the dashed line separates the heavy from the light fragments by equal amount.

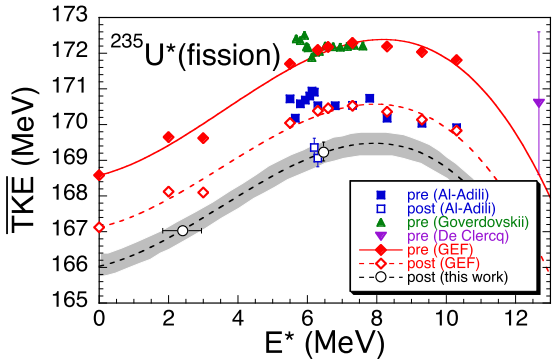

FIG. 4. Overview of $\overline{\text{TKE}}$ of fission fragments for different excitation energies in ^{235}U. Filled and open symbols indicate values "pre" and "post" neutron emission, respectively. Experimental data from Refs. [9,15,17,18] in descending order are compared to results from GEF calculations [20]. These points are fitted with third-order polynomials for "pre" and "post"; the latter is then shifted to match the results from this work, depicted as open circles.

tation energy equal to the energy of the superdeformed ground state E_{II}. For direct, i.e., prompt, fission of ^{235}U*, induced by neutrons [9,17] and bremsstrahlung photons of 25 MeV endpoint energy [18], $\overline{\text{TKE}}$ was determined for different excitation energies. For the latter, an average excitation energy was estimated by weighting a simulated bremsstrahlung spectrum with the ^{235}U(γ, f) cross section from Ref. [19]. Hence, analyzing the variation of $\overline{\text{TKE}}$ with excitation energy should allow assignment of a value for E_{II} from the observed $\overline{\text{TKE}}$ for isomeric fission. The above-mentioned experimentally determined $\overline{\text{TKE}}$ data [9,17,19] as a function of E^* is depicted in Fig. 4, for fragments prior to neutron emission denoted with "pre" and indicated with filled symbols. Post-neutron emission $\overline{\text{TKE}}$ values from Ref. [15] are denoted with "post" and depicted as open squares. In order to assess the energy dependence down to $E* = 0$ MeV, calculations were performed with the model code GEF [20], providing a general description of fission observables. These calculations were performed for ^{235}U(sf) at $E^* = 0$ MeV, ^{234}U(n, f) for $E^* > S_n$, and ^{235}U(γ, f) in between. The results—pre- and post-neutron emission—are depicted as full and open diamonds, respectively, as well as solid and dashed lines, which correspond to fitted third-order polynomials.

Obviously, the GEF calculations provide a good description of the experimental values from Ref. [17], which however are 1.75 MeV too high due to a revised reference value [9]. Correcting for that gives a good agreement between the data of Refs. [9] and [17]. Apart from this discrepancy, the energy dependence according to GEF agrees rather well with data from Ref. [9] for $\overline{\text{TKE}}$(pre). Hence, the same is assumed for the calculated $\overline{\text{TKE}}$(post) dependence, which is adjusted to the experimental data from Ref. [15], resulting in the darker (i.e., black) dashed line. Due to the energy calibration of the pulse height spectra from this work, the $\overline{\text{TKE}}$(post) for prompt fission at $E^* = \overline{E}_n + S_n = 6.46$ MeV, depicted as open circle, lies on this line. The systematic uncertainty of 0.3 MeV (see above) defines the shaded uncertainty band. The corresponding value for isomeric fission, $\overline{\text{TKE}}$(post) = (167.0 ± 0.3) MeV, should be situated on the black dashed line, resulting in $E^* =: E_{II} = (2.4 \pm 0.6)$ MeV. The uncertainty here is estimated by the width of the shaded area in horizontal direction (see Fig. 4). Below all results are summarized; they will later be interpreted in terms of fission modes and their impact on further barrier parameters will be discussed.

TABLE I. Experimental results from this work for both incident neutron energies as well as combined for the average energy $\overline{E}_n = 1.16$ MeV, compared to previous ones [7]. All uncertainties are statistical ones unless noted. See text for more details.

	This work			
E_n (MeV)	0.95	1.27	1.16	Ref. [7]
$T_{1/2}$ (ms) [a]			11 ± 3	3.6 ± 1.8
N_{iso}	36 ± 8	46 ± 10	79 ± 10	
N_{prompt} ($\times 10^6$)	2.73	5.30	8.03	
P_{iso} ($\times 10^{-6}$)	13 ± 3	9 ± 2	10 ± 1	7.5 ± 6.0
$\sigma_{n,f}$ (b) [b]	1.08	1.25	1.19	
σ_{iso} (μb)	14 ± 3	11 ± 3	12 ± 1	10 ± 8
E_{II} (MeV)			2.4 ± 0.6	

[a]The deduced half-life of the shape isomer is kept constant, introducing systematic uncertainties of 5 and 6 on N_{iso} for $E_n = 0.95$ and 1.27 MeV, respectively, which propagates.
[b]Cross sections are taken from Ref. [22].

IV. RESULTS

The primary results from the analysis of both time and pulse height data related to the shape isomer in ^{235}U are collected in Table I. For comparison previous results as given in Ref. [7] are listed as well. The overall agreement—whenever possible—is good, except for the deduced half-life for isomeric decay. This is due to the new and different treatment of the decay data, which indeed has proven to be advantageous in terms of precision, especially when the deduced half-life is similar to the measured time range. Still, within two σ the uncertainties of both values overlap. The most striking difference, however, is the higher precision of the new results. Below they will be discussed and, by using additional data from both experiment and theory, parameters describing the fission barrier will be deduced.

V. DISCUSSION

The results presented above for $T_{1/2}$ and E_{II} may be used to to extract information about the outer fission barrier according to the Hill-Wheeler approximation [3],

$$T_{1/2} = 2.77 \times 10^{-21} \exp\left[2\pi (E_B - E_{II})/\hbar\omega_B\right]. \quad (3)$$

Here E_B and $\hbar\omega_B$ denote the height and penetrability (i.e., width) of the outer barrier, respectively. All energies are given in MeV, while $T_{1/2}$ is given in s. Combining our results with $E_B = (5.6 \pm 0.3)$ MeV [3] and (6.0 ± 0.3) MeV [6] leads to $\hbar\omega_B = (0.47 \pm 0.10)$ MeV and (0.53 ± 0.10) MeV, respectively. Using the recommended value $\hbar\omega_B = 0.52$ MeV [5] leads to a barrier height of $E_B = 5.9$ MeV. Obviously, a decision about which combination to choose cannot be made

only based on our results, only that E_B and $\hbar\omega_B$ are connected according to Eq. (3), leading to the relation

$$E_B = (6.816 \pm 0.043)\,\hbar\omega_B + (2.4 \pm 0.6)\ \text{MeV}. \quad (4)$$

Hence, more information is necessary, which, however, is already available elsewhere. In order to use this information we interpret our experimental observations in terms of fission modes [21].

From the experimental values for $\overline{\text{TKE}}$(pre) and $\overline{\text{TKE}}$(post) from Ref. [9] together with the results of the GEF calculations, we can estimate $\overline{\text{TKE}}$(pre) corresponding to our $\overline{\text{TKE}}$(post) values for prompt and isomeric fission by adding the difference between the two fits to GEF data (solid and dashed lines; see Fig. 4) at the appropriate excitation energies. Accordingly, we obtain $\overline{\text{TKE}}_{\text{iso}}$(pre) $\approx$ 168.6 MeV and $\overline{\text{TKE}}_{\text{prompt}}$(pre) $\approx$ 170.7 MeV. This makes perfect sense, since lower $\overline{\text{TKE}}$ values indicate a longer prescission shape [21], corresponding to a larger deformation of the system until passing the fission barrier and eventually scission, which indeed is the case for isomeric fission. This picture is consistent in terms of fission modes, which correspond to different paths in the potential energy landscape leading to fission. At excitation energies for prompt fission like in this work, three fission modes have been observed [9], each related to a specific prescission shape leading to a characteristic mass and TKE distribution. Those modes are the two asymmetric standard-1 (S1) and standard-2 (S2) modes, of which S2 with a higher degree of asymmetry and lower $\overline{\text{TKE}}$ is dominating by about 4 to 1. The third mode, leading to a symmetric mass distribution with even lower $\overline{\text{TKE}}$, is called superlong (SL), which however contributes here only with at most about 1% [9]. There we find $\overline{\text{TKE}}_{S1} \approx 182$ MeV and $\overline{\text{TKE}}_{S2} \approx 168$ MeV, while $\overline{\text{TKE}}_{SL} \approx 155$ MeV may be inferred from Ref. [21]. For prompt fission ($E^* = 6.5$ MeV), $\overline{\text{TKE}} \approx 170.7$ MeV, which corresponds to about 18% S1 and 82% S2 [9]. For isomeric fission ($E^* \approx 2.4$ MeV), $\overline{\text{TKE}} \approx 168.8$ MeV, which allows in principle two possible explanations: (*i*) a considerable contribution of SL, or (*ii*) an enhanced contribution of S2 without SL. However, the first possibility may be ruled out by comparison with observations from the similar system ^{236}U, in which no increase of symmetric fission was observed in the fragment mass distribution from isomeric fission compared to prompt fission [5]. Hence, $\overline{\text{TKE}}_{\text{iso}}$ may be explained by practically S2 alone (about 3% S1 and 97% S2). In reverse, studying isomeric fission of ^{235}U seems to offer an excellent opportunity to obtain pure information about the standard-2 mode.

Since mode weights [9] as well as the cross section [22] for ^{234}U(n, f) are known, we may employ a procedure previously applied to, e.g., ^{238}U(n, f) [23] and ^{237}Np(n, f) [24] to extract information on barrier parameters. In an extended approximation, taken from Refs. [3,5] and ignoring any SL contribution, the fission cross section may be expressed as

$$\sigma_f = \sum_i \sigma_{f,i} = \sum_i \sigma_{0,i} \times T_A\, T_B/(T_A + T_B), \quad (5)$$

where i = S1,S2 and $\sigma_{f,i}$ denotes the mode-weighted cross-section data. The transmission through the individual barriers

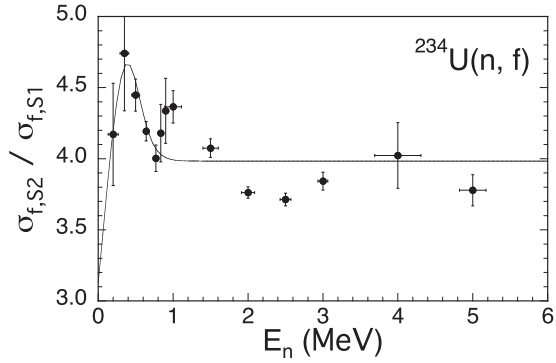

FIG. 5. Ratio of mode-weighted cross sections for S1 and S2 for the reaction ^{234}U(n, f) in the energy range E_n = 0.2–5.0 MeV (black dots) together with the result of a fit according to Eqs. (5) and (6) (line). The cross section values were taken from Ref. [22], while the mode weights were taken from Ref. [9].

$X = A, B$ is given by

$$T_X(E_n) = [1 + \exp\{2\pi(E_X - E_n - S_n)/\hbar\omega_X\}], \quad (6)$$

approximating the barriers by inverted parabola segments of height E_X and width $\hbar\omega_X$ [25]. E_n and $S_n = 5.289$ MeV [5] denote incident neutron energy and neutron separation energy, respectively. Figure 5 shows the ratio of the mode-weighted cross sections and the result from the fit according to Eqs. (5) and (6) in the energy range E_n = 0.2–5.0 MeV. Here, the parameters describing the inner barrier were not fitted, but adopted from Ref. [3], p. 30, as $E_A = (5.9 \pm 0.2)$ MeV and $\hbar\omega_A = 0.8$ MeV. Assuming a common inner fission barrier for both S1 and S2 mode is justified by theoretical predictions [21] as well as the previous treatment of experimental data [23,24], among others. Moreover, in order to facilitate a converging fit, $\sigma_{f,S2}(E_n)$ was fitted first and the results for $E_{B,S2}$ and $\hbar\omega_{B,S2}$ were kept when fitting the ratio $\sigma_{f,S2}(E_n)/\sigma_{f,S1}(E_n)$. The results are $E_{B,S1} = (5.83 \pm 0.07)$ MeV and $\hbar\omega_{B,S1} = (0.57 \pm 0.03)$ MeV as well as $E_{B,S2} = (5.77 \pm 0.07)$ MeV and $\hbar\omega_{B,S2} = (0.48 \pm 0.03)$ MeV, as listed below in Table II.

The results obtained, in particular those for S2, may be compared with the relation according to Eq. (4), since the observed value for $\overline{\text{TKE}}_{\text{iso}}$ may be explained by the value for S2 only. In Fig. 6, Eq. (4) is represented by a line together with a shaded band to indicate the uncertainties. The open circle denotes the combination from the fit of the mode-weighted cross section for S2, distinguished by the dashed crosshair. Best agreement, i.e. the closest distance between this point and a point on the line is realized by minimizing the residual sum of squares, leading to $E_B = (5.7 \pm 0.6)$ MeV and $\hbar\omega_B = (0.5 \pm 0.1)$ MeV. These values, too, are summarized in Table II.

VI. SUMMARY AND CONCLUSIONS

In this work we have revisited the shape isomer in ^{235}U. By reanalyzing previously taken data leading to the identification of the shape isomer [7], and combining this with recently measured fission fragment properties from the reac-

TABLE II. Fission barrier parameters of ^{235}U, obtained in this work and compared to previously published values from Bjørnholm and Lynn [3], Weigmann and Theobald [6], Wagemans [5], Tudora *et al.* [26], and RIPL-3 [27]. In addition to an average outer barrier, values for extracted mode-dependent barrier parameters for S1 and S2 are given. In this work values from Ref. [3] were assumed to describe the inner barrier.

				E_B (MeV)		$\hbar\omega_B$ (MeV)	
Reference	E_A (MeV)	$\hbar\omega_A$ (MeV)	E_{II} (MeV)	S1	S2	S1	S2
This work			2.4 ± 0.6	5.7 ± 0.6		0.5 ± 0.1	
This work			2.4 ± 0.6	5.83 ± 0.07	5.77 ± 0.07	0.57 ± 0.03	0.48 ± 0.03
Ref. [3]	5.9 ± 0.2	0.8	2.5 ± 0.3	5.6 ± 0.2		0.52	
Ref. [3]	6.15	0.8		5.92		0.52	
Ref. [6]	5.97	1.44	2.55	5.93		–	
Ref. [5]	5.9	0.8	2.5	5.6		0.52	
Ref. [26]	4.8	0.8	2.0	5.855		0.45	
Ref. [27]	5.25	0.7	–	6.0		0.5	

tion ^{234}U(n, f) [8,9], information on the fission barrier could be extracted. The half-life for the decay of the shape isomer was determined as $T_{1/2} = (11 \pm 3)$ ms, which is about three times longer than reported before [7], but still overlapping within 2σ uncertainties. This difference is explained by an improved analysis method of the measured time distribution of the isomeric fission events, i.e., by applying a so-called ^{2}log-scale binning [10]. This turned out to be advantageous, because the experimentally covered time range was actually not much longer than the hitherto unknown half-life. The new value is not only more reliable, but also of less uncertainty. From our analysis we conclude that future half-life measurements of this isomer should cover a time range of at least 100 ms. The cross section obtained for isomeric fission, $\sigma_{\text{iso}} = (12 \pm 1)$ μb, is in agreement with the previous result of (10 ± 8) μb [7].

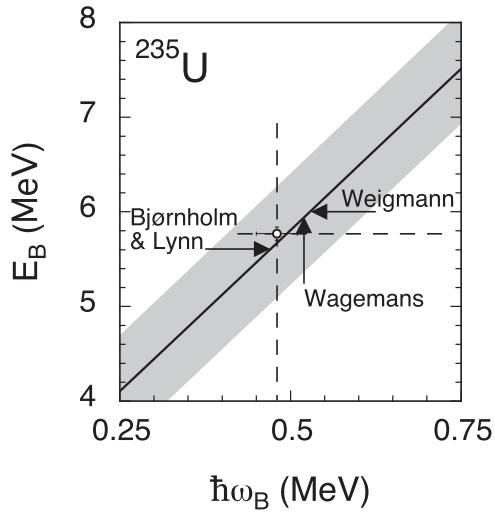

FIG. 6. Overview of possible parameters describing the outer fission barrier of ^{235}U. The solid line corresponds to the relation between E_B and $\hbar\omega_B$ according to Eq. (4) with depicted uncertainties as shaded area. The open circle, emphasized with a dashed crosshair, denotes the combination for S2 obtained from the mode-weighted cross sections. In addition, published values from Refs. [3,5,6] are indicated by arrows.

Studying the excitation-energy dependence of the average total kinetic energy of the fission fragments, $\overline{\text{TKE}}(E^*)$, allowed estimation of the energy of the super-deformed ground state of ^{235}U to $E_{II} = (2.4 \pm 0.6)$ MeV. This result, albeit with a considerable uncertainty, is in good agreement with various predicted values [3,5,6,26,27] (see Table II). Moreover, from level spacings of class-I and class-II states, $D_I = (10.6 \pm 0.5)$ eV and $D_{II} = (2.1 \pm 0.3)$ keV [28], respectively, together with a level density parameter $a = 26.68$ MeV^{-1} [27], a value of $E_{II} = (2.35 \pm 0.06)$ MeV may be deduced (see Ref. [5], Chap. 4), which is also in excellent agreement with the result of our work. The interpretation of $\overline{\text{TKE}}(E^*)$ in terms of fission modes [21] gave strong indications that isomeric fission proceeds almost exclusively via the standard-2 mode. Hence, according to our findings, fragments from isomeric fission of ^{235}U should reveal quite clean information about characteristics of this fission mode. Whether this applies to other compound systems as well, remains to be investigated.

From the values for $T_{1/2}$ and E_{II} obtained so far, a relation between parameters describing the outer fission barrier, E_B and $\hbar\omega_B$, could be found. In order to narrow down possible combinations, we have even analyzed mode-weighted cross sections for ^{234}U(n, f), with mode weights from Ref. [9] and cross section values from Ref. [22]. Hereby we assumed parameters from Ref. [5] for the inner fission barrier. The results for the outer barrier, an average height $E_B = (5.7 \pm 0.6)$ MeV and a curvature $\hbar\omega_B = (0.5 \pm 0.1)$ MeV, imply that both barriers have about the same height. Corresponding values were deduced for the outer barriers for S1 and S2 modes, which are supposed to have a common inner barrier. All this is in good agreement with values in Refs. [3,5,6], but contradicts recent results from model calculations [26,29]. The latter assumes a triple-humped barrier, but both suggest an inner barrier height $E_A = 4.80$ MeV. However, this would lead to a probability for γ decay back to the inner well that is three orders of magnitude higher than the one for isomeric fission. In contrast, applying the barrier parameters for the inner barrier used in

this work and those for the outer barrier estimated here gives a ratio of 0.33. This corresponds to a ratio of partial half-lives

$$\frac{T_{1/2}(i\gamma)}{T_{1/2}(if)} \approx 3 \tag{7}$$

with $T_{1/2} = [T_{1/2}(i\gamma)^{-1} + T_{1/2}(if)^{-1}]^{-1}$. Here, the subscripts $i\gamma$ and if stand for γ decay and isomeric fission, respectively. This is in good agreement with values for other uranium isotopes (see Ref. [5], p. 48). With this ratio and the half-life determined in this work, $T_{1/2} = 11$ ms, one may estimate the partial half-lives $T_{1/2}(\text{if}) \approx 14.7$ ms and $T_{1/2}(i\gamma) \approx 44$ ms. Inserting $T_{1/2}(if)$ instead of $T_{1/2}$ in Eq. (3) changes the coefficient in Eq. (4) from 6.816 to 6.862, which, however, has no significant impact on the deduced outer fission-barrier parameters.

In conclusion, we show here that the measurement of the life-time of a shape isomer together with certain fission fragment properties, like cross sections, mode weights and average total kinetic energy, allows extraction of fission barrier parameters that give a consistent picture. The parameters obtained for ^{235}U explain the observed half-life of the isomer, and why it is difficult to observe γ decay of the fission isomer. Since the value of E_{II} corresponds to the mass difference of ^{235}U in the super-deformed and the normal ground state, respectively, the uncertainty of E_{II} is expected to become smaller in such a dedicated measurement. Future work is therefore planned.

ACKNOWLEDGMENTS

One of the authors (A. O.) acknowledges the support from the Extreme Light Infrastructure Nuclear Physics (ELI-NP) Phase II, a project co-financed by the Romanian Government and the European Union through the European Regional Development Fund, the Competitiveness Operational Programme (1/07.07.2016, COP, ID 1334), with which part of this work had been performed.

[1] V. M. Strutinsky, Nucl. Phys. A **95**, 420 (1967).
[2] R. Vandenbosch, Annu. Rev. Nucl. Sci. **27**, 1 (1977).
[3] S. Bjørnholm and J. E. Lynn, Rev. Mod. Phys. **52**, 725 (1980).
[4] P. Thirolf and D. Habs, Prog. Part. Nucl. Phys. **49**, 325 (2002).
[5] *The Nuclear Fission Process*, edited by C. Wagemans (CRC, Boca Raton, FL, 1991).
[6] H. Weigmann and J. P. Theobald, Nucl. Phys. A **187**, 305 (1971).
[7] A. Oberstedt, S. Oberstedt, M. Gawrys, and N. Kornilov, Phys. Rev. Lett. **99**, 042502 (2007).
[8] A. Al-Adili, Ph.D. thesis, Uppsala University, 2013 (unpublished), http://uu.diva-portal.org/smash/get/diva2:573126/FULLTEXT01.pdf.
[9] A. Al-Adili, F.-J. Hambsch, S. Pomp, S. Oberstedt, and M. Vidali, Phys. Rev. C **93**, 034603 (2016).
[10] H. Bartsch, K. Huber, U. Kneißl, and H. Sattler, Nucl. Instrum. Methods **121**, 185 (1974).
[11] V. Metag, R. Repnow, and P. von Brentano, Nucl. Phys. **165**, 289 (1971).
[12] V. Metag, in Ref. [5], p. 49 ff.
[13] Z. Ren and C. Xu, Nucl. Phys. **759**, 64 (2005).
[14] E. Birgersson, Ph.D. thesis, Örebro University, 2007 (unpublished), http://oru.diva-portal.org/smash/get/diva2:135073/FULLTEXT01.pdf.
[15] A. Al-Adili (private communication).
[16] A. Azzalini, Scand. J. Statist. **12**, 171 (1985).
[17] A. A. Goverdovskii, B. D. Kuzminov, V. F. Mitrofanov, and A. I. Sergachev, Sov. J. Nucl. Phys. **44**, 179 (1986).
[18] A. De Clercq, E. Jacobs, D. De Frenne, H. Thierens, P. D'hondt, and A. J. Deruytter, Phys. Rev. C **13**, 1536 (1976).
[19] J. T. Caldwell, E. J. Dowdy, B. L. Berman, R. A. Alvarez, and P. Meyer, Phys. Rev. C **21**, 1215 (1980).
[20] K.-H. Schmidt, B. Jurado, C. Amouroux, and C. Schmitt, Nucl. Data Sheets **131**, 107 (2016).
[21] U. Brosa, S. Grossmann, and A. Müller, Phys. Rep. **197**, 167 (1990).
[22] ENDF/B-VIII.0 Evaluated Nuclear Data Files (2018), ZA=92234, NSUB=7, MT=19, MF=3, https://www.nndc.bnl.gov/.
[23] S. Oberstedt, F.-J. Hambsch, and F. Vivès, Nucl. Phys. **644**, 289 (1998).
[24] F.-J. Hambsch, F. Vivès, P. Siegler, and S. Oberstedt, Nucl. Phys. **679**, 3 (2000).
[25] D. L. Hill and J. A. Wheeler, Phys. Rev. **89**, 1102 (1953).
[26] A. Tudora, F.-J. Hambsch, and S. Oberstedt, Nucl. Phys. **917**, 43 (2013).
[27] Reference Input Parameter Library (RIPL-3), https://www-nds.iaea.org/RIPL-3/.
[28] G. D. James, J. W. T. Dabbs, J. A. Harvey, N. W. Hill, and R. H. Schindler, Phys. Rev. C **15**, 2083 (1977).
[29] M. Sin, R. Capote, M. W. Herman, and A. Trkov, Nucl. Data Sheets **139**, 138 (2017).